INNOVATIVE STRUCTURAL ELEMENTS OF SUPER HIGH STRENGTH AND DUCTILITY

Kulsiri Chandrangsu-Ferrand, PhD, Post-doctoral fellow, Dept. of Civil Engineering, University of Michigan, Ann Arbor, MI
Antoine E. Naaman, PhD, Professor, Dept. of Civil Engineering, University of Michigan, Ann Arbor, MI

ABSTRACT

This study describes an innovative structural concept which can be immediately applied to new concrete bridges with the potential to lead to significantly higher strength, ductility, and durability. In this proposed concept, unstressed prestressing strands are used as primary reinforcement in a high performance fiber reinforced cement (HPFRC) composite flexural beam. By taking advantage of the high compressive strength, strain capacity, and strain-hardening behavior of HPFRC matrix, as well as the high tensile strength of steel strands, a flexural performance better than that of conventional reinforced concrete beam is expected. This paper describes the preliminary phase of this research which deals with laboratory testing of six beams designed according to the above concept. The experimental program included the testing of 10 ft. long simple span T-beams and two-span continuous rectangular beams. Experimental results described here focus on inelastic behavior, serviceability (cracking), energy absorption, the formation of plastic hinges, and comparison with the control specimens. Based on the findings, significantly higher strength and ductility are observed in comparison to conventional reinforced concrete. Moreover significantly smaller crack widths are achieved implying considerably better long-term durability.

Keywords: Fiber, Prestressed concrete, Flexural behavior, Strain-hardening behavior, Plastic hinges, Energy absorption, Ductility

INTRODUCTION

It is generally agreed that today's functionality of a significant proportion of US infrastructure, such as bridges, is barely at the minimum acceptable performance level. This is likely to be true in other countries as well. The maintenance of bridges consumes a significant fraction of available maintenance funds in the US. Under normal usage and wear-and-tear, most bridges show significant deterioration. Under extreme load conditions, such as earthquake, total collapse and loss of life has been reported. This is due in great part to the limited capability of conventional construction materials and structural systems used to date.

Over the past two decades, a new generation of fiber reinforced cement composites has been developed. They are identified as "High Performance Fiber Reinforced Cement Composites (HPFRCC)" and are characterized by a tensile stress-strain response that exhibits pseudo strain hardening accompanied by multiple cracking, as shown in Fig. 1. It is strongly believed that high performance fiber reinforced cement composites (HPFRCC) are emerging materials well suited for use in the next generation of infrastructure. HPFRCCs can be tailored-designed to prescribe strength, toughness, durability, ductility, and fracture energy [1, 2, 3]. In previous research work [4, 5], HPFRCCs are reported to develop high compressive strengths as well as large strains prior to failure in compression. That is equivalent to say that, for the same strength, they show significantly higher ductility than concrete without fibers. In addition, high-strength steel strands as well as carbon fiber reinforced polymeric bars (CFRP) with high tensile strength are readily available on the market today. By combining these two materials in a typical reinforced concrete beam and taking advantage of their improved properties, analytical predictions suggest that such reinforcing systems would carry at least two times the load of a conventional reinforced concrete beam, while also providing at least two times the energy absorption capacity and related ductility. The crack width limit state as well as other serviceability limit states, such as deflection, would also remain non critical.

Therefore, the main objective of this study was to evaluate experimentally the above concept. This paper mainly describes the preliminary phase of this research which deals with laboratory testing of six beams. The experimental program included the testing of three 10 ft-long simple span T-beams and 3 two-span continuous rectangular beams. The next phase which includes field implementation in the construction of a real bridge is hoped for, depending on future funding.

RESEARCH SIGNIFICANCE

The use of high strength steel/CFRP bars in conventional reinforced concrete has been limited because the tensile strength of the reinforcement could not be fully utilized and because the strain capacity of concrete in compression is insufficient. In the case of FRP reinforcements the brittleness of the reinforcement itself and its poor dowel resistance add additional constraints. Moreover when the stress in the reinforcement under service load is allowed to increase, the width of cracks in concrete increases, and the crack width limit state may be violated. The use of HPFRC composites to replace conventional concrete takes care

of most of the above drawbacks, namely increased strain capacity of concrete in compression, allowing much higher strengths and allowable stresses in the reinforcement, and decreased crack widths thus improving durability. Indeed, there is a compelling need to develop new structural systems with increased performance particularly related to high strength, high ductility and durability. In this study a solution that can be implemented immediately with current materials and technology while satisfying existing codes (i.e. ACI, AASHTO, etc.), is provided.

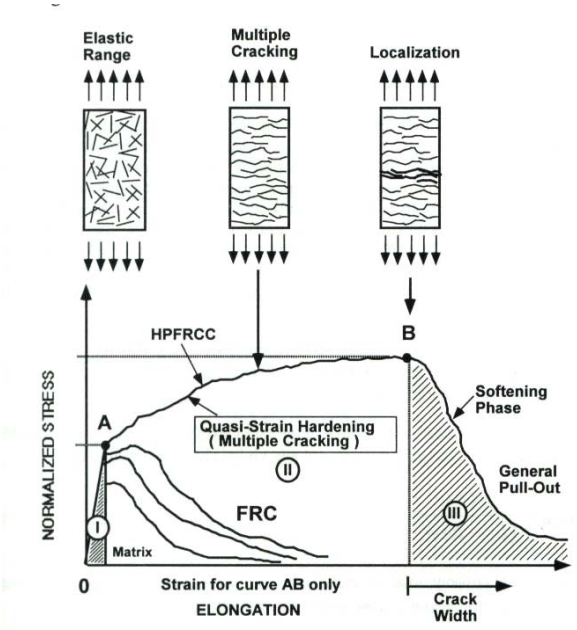

Fig. 1 Characteristic of high performance fiber reinforced composites

EXPERIMENTAL PROGRAM

TEST SPECIMENS

The experimental program consisted in the testing of 6 specimens; 3 simple span T-beams (identified as Group 1) and 3 two-span continuous rectangular beams (identified as Group 2). The first group was chosen to verify the feasibility of the proposed concept and develop data on the moment-curvature of HPFRC composites sections reinforced with prestressing strands. Group 2 was also chosen to verify the proposed concept for continuous spans and to study the rotation over the intermediate support and evaluate the length of the plastic hinge there. All specimens are 10 ft. long. Their cross sections are shown in Figures 2(a) and (b) for specimens in Group 1 and Group 2, respectively. For the control beams in each group, conventional concrete was used. For the proposed beams, the HPFRC matrix was achieved with a cement mortar reinforced with Torex steel fibers. The Torex fiber is a new type of deformed steel fiber polygonal in cross section and twisted along its longitudinal axis; as shown in Fig. 3. It was first introduced in 1998 by A.E. Naaman [6, 7].

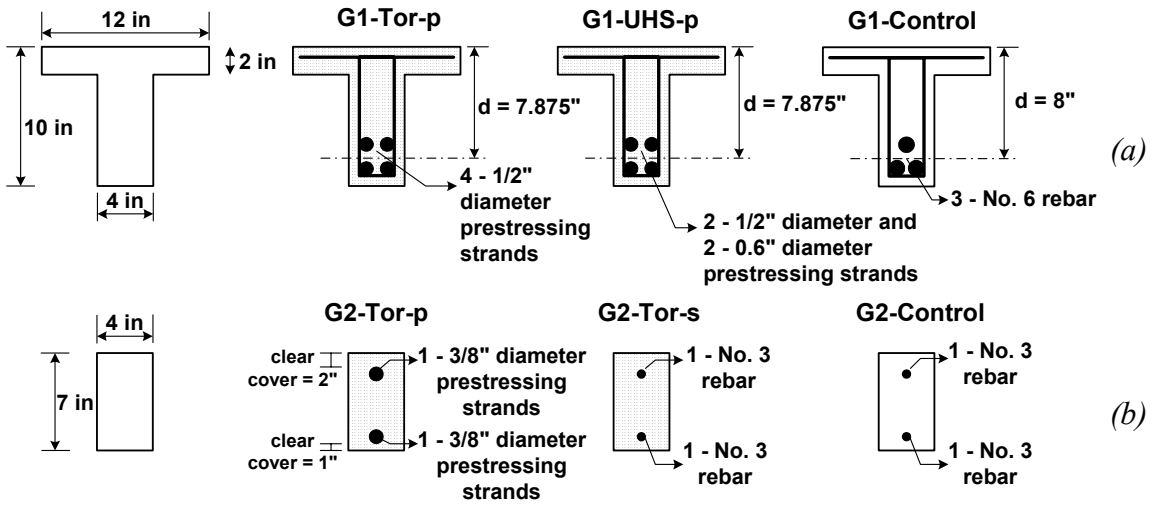

Fig. 2 Test specimens (a) Specimen in group 1 (b) specimen in group 2

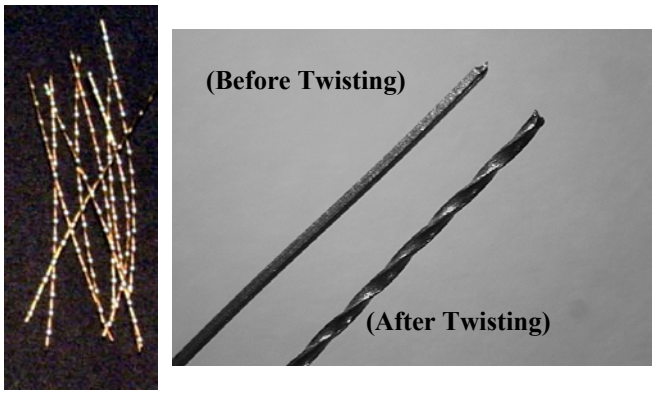

Fig. 3 Typical Torex fiber used to produce HPFRC composites

In the first group, three specimens were cast with 3 different matrices. The first specimen, identified as G1-Tor-p, represents the proposed beam with 2% Torex fiber reinforced mortar reinforced with prestressing strands. The second specimen, identified as G1-UHS-p, represents the proposed beam with ultra high strength mortar which contained 2.5% Torex fibers reinforced with prestressing strands. And, the third specimen, identified as G1-Control, represents a conventional reinforced concrete beam made of normal concrete and reinforcing bars.

Similarly, the first specimen in group 2, identified as G2-Tor-p, represents the proposed beam with HPFRCCs reinforced with prestressing strands, and the second specimen in group 2, identified as G2-Tor-s, represents the beam with HPFRCCs reinforced with conventional steel rebars. The third specimen in group 2, identified as G2-Control, represents a standard reinforced concrete beam made of conventional concrete and reinforcing bars. Table 1 shows the characteristics of each test beam in this experimental program.

Table 1 Characteristic of test specimens

Group	ID	Type of test	Cross-section	Type of matrices	Type of reinforcements
1	G1-Tor-p	Simple span	T-shape	2% Torex fibers reinforced mortar	Prestressing strands
	G1-UHS-p			Ultra high strength mortar with 2.5 % Torex fibers	Prestressing strands
	G1-Control			Conventional concrete mix	Reinforcing bars
2	G2-Tor-p	Continuous span	Rectangular	2% Torex fibers reinforced mortar	Prestressing strands
	G2-Tor-s			2% Torex fibers reinforced mortar	Reinforcing bars
	G2-Control			Conventional concrete mix	Reinforcing bars

Specimens in group 1 were designed to be closed to the maximum limit of tension controlled section ($\varepsilon_t = 0.005$) according to the ACI code [8]. This implies that the section would have a value of c/d close to 0.375, thus the section would behave as a T-section and reinforcements in the specimens would also yield shortly before specimen fails by crushing of concrete at the top fiber. For specimens with HPFRC composites, nonlinear analysis was performed in order to design the specimens to be closed to maximum limit of tension controlled section and the effect of HPFRC matrices was incorporated in the design through the input of stress-strain relationships of HPFRC matrices in the nonlinear analysis. Note that these stress-strain relationships were obtained experimentally from material testing of HPFRC composites.

For group 2, the control specimen was designed to have low reinforcement ratio. The reinforcement in specimens with HPFRC matrix (G2-Tor-s and G2-Tor-p) was then kept the same as in the reference beam to evaluate the effect of fiber and the type of reinforcement. Similar to specimens in group 1, section nonlinear analysis was used for the design of specimens with HPFRC matrix to achieve the mentioned criteria.

MATERIAL PROPERTIES

Three types of matrices were used in this study, 2 types of HPFRC composites for the proposed beams, and 1 conventional concrete mix for the control beams. Details on mixture proportions are given in Table 2. Note that the compressive strength of the ultra high strength (UHS) mix is the highest, followed by 2% Torex fiber reinforced mortar, and conventional concrete has the lowest strength.

Two types of Torex fibers were used to produce HPFRC matrices in this study. Fiber properties are shown in Table 3.

The main reinforcement consisted of either 7-wire steel prestressing strands or conventional steel reinforcing bars. Their properties are given in Table 4.

Table 2 Composition by weight and properties of matrices used in this study

Type of matrices	Mix Proportion by weight		Compressive strength, f'c ksi **
Mortar with 2% Torex fibers (Tor)	Cement Type III	1	8.6
	Flint sand	1	
	Fly ash class C	0.15	
	Water	0.4	
	Superplasticizer	0.003	
	Torex fiber no. 1*	2% by volume	
Ultra high strength mortar with 2.5% Torex fibers (UHS)	Cement Type III	1	14.1
	Silica fume	0.24	
	270 sand	0.38	
	Flint sand	1.1	
	Water	0.27	
	Superplasticizer	0.1	
	Retarder	0.005	
	Torex fiber no. 2*	2.5% by volume	
Concrete mix (Control)	Ready-mix		4.8

*As shown in Table 3

** From capped cylinder (∅ 4 in. and 8 in. high)

Table 3 Properties of Torex fibers used in this research

Fiber Type	Diameter, in (mm)	Length, in (mm)	Cross-sectional shape	Tensile Strength**, ksi (MPa)	Elastic Modulus, ksi (GPa)
Torex No. 1	0.012 (0.3)*	1.18 (30)	Rectangular	360 (2470)	29000 (200)
Torex No. 2	0.020 (0.5)*	1.38 (35)	Triangular	260 (1800)	29000 (200)

* Equivalent diameter

** From tensile test of twisted wire

Table 4 Mechanical properties of reinforcements used in the test program

Type	Yield strength, ksi (MPa)	Elastic Modulus, ksi (GPa)	Ultimate tensile strength, ksi (MPa)	Ultimate strain, (%)
Reinforcing steel*	68 (470)	29000 (200)	85 (587)	14
Prestressing strand**	243.5 (1679)	28000 (186)	270 (1862)	6.9

* Nominal values obtained from tensile test of rebar

** Data from manufacturer

TESTING AND INSTRUMENTATION

Figures 4(a) and (b) shows the test setup used in this experimental program. In case of a simple span beam, two point loads were 2 ft. apart and were applied at 4 ft. away from each support. In case of a continuous beam, each span is 5 ft. long. Two point loads were 3.75 ft. apart and were applied at 3.125 ft. away from each exterior support. A servo-hydraulic Instron machine was used as well as LVDTs and clinometers to record special measures. In a case of simple span beams, three LVDTs were used to measure the displacement of the specimen, one at midspan, one under each load point. Two clinometers were used to measure the curvature of the specimen at midspan and will eventually be used to verify the accuracy of the analytical model. In a case of continuous beams, Two LVDTs were used to measure the displacement of the specimen under each load point. To study the rotation over the intermediate support, four LVDTs were used to measure the rotation of the specimen at intermediate support over a length of 8 in.: two at the top fiber and two at the bottom fiber of the section. The rotation was calculated from the summation of the change in length at the top fiber and the change in length at the bottom fiber divided by the overall height of the section. In this paper, the rotation is presented in percent of radian.

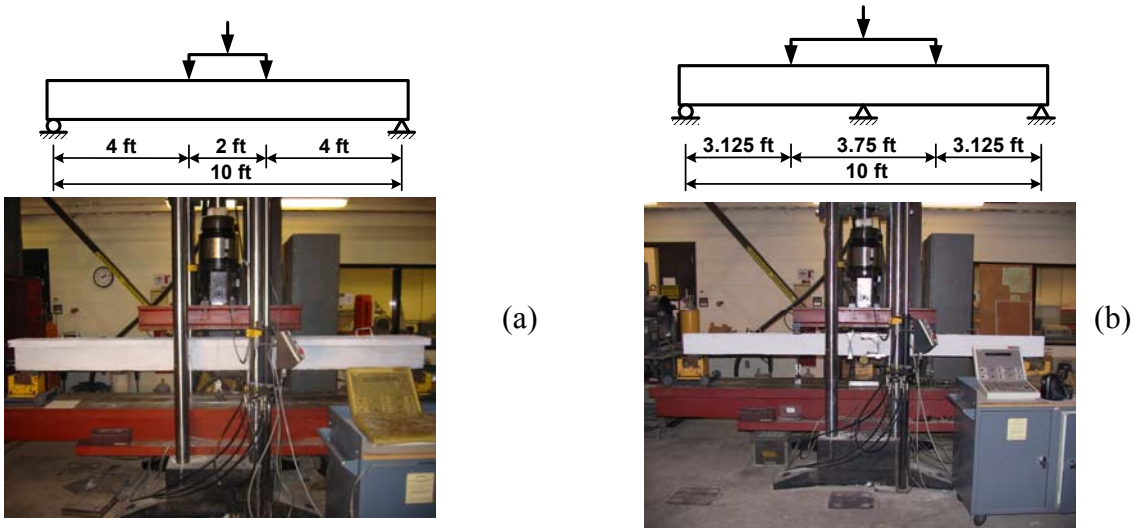

Fig. 4 Test setup (a) simple span configuration for specimens in group 1 (b) continuous span configuration for specimen in group 2

EXPERIMENTAL RESULTS

The behavior of tested specimens is discussed in this section. First, results from specimens in group 1 will be presented, followed by the results from specimen in group 2.

TEST RESULTS OF SIMPLE SPAN BEAMS

Load-Deflection Responses

Fig. 5 shows the load versus deflection curves of test specimens in group 1. Also, Table 5 presents the summary of the numerical results obtained from these specimens. Initially, all specimens behaved elastically up to cracking. Cracking load reported here corresponds to the point at which the initial portion of the load-deflection curve starts to deviate from linearity. Proposed specimens with HPFRC matrices show slightly higher cracking load compared to control specimen with conventional concrete, of which specimen with UHS mix shows the highest cracking load, due to its higher modulus of rupture.

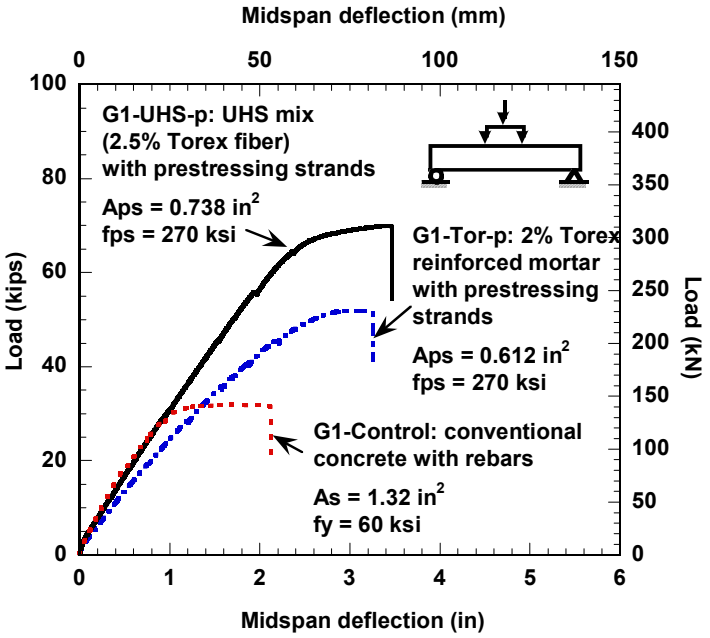

Fig. 5 Comparison of load-deflection curves of simple-span test specimens

Table 5 Summary of the numerical results obtained from tested specimens in group 1

Specimen ID	Cracking load (kips)	Corresponding deflection at cracking (in)	Peak load (kips)	Corresponding midspan deflection (in)	Total energy absorption (kip-in)
G1-Tor-p	3.58	0.129	51.96	3.02	111.24
G1-UHS-p	4.61	0.092	69.99	3.44	158.12
G1-Control	2.52	0.039	32	2.08	55.71

Loading – unloading was also done periodically during the beginning of the test to investigate the inelastic behavior and serviceability of the proposed beams. Fig. 6 shows the loading-unloading responses of specimen with UHS mix compared to the control specimen. Unloading at the load of about 9 and 18 kips (30% and 60% of the predicted maximum load of the control specimen) shows slightly permanent deflection in all specimens. As shown in

Fig. 6, even though the control specimen has higher stiffness due to its higher amount of reinforcement, the proposed specimen exhibited the same magnitude of permanent deflection. In addition, unloading was also carried out at the load of 30 kips for specimen with UHS mix. At this load level, the reinforcement in the control specimen already yielded which would result in a large permanent deflection when unloading. However, as shown in Fig. 6(a), it can be seen that very small permanent deflection (less than L/600) was observed in the specimen with UHS mix after unloading. This is due to the effect of fiber bridging in the HPFRC matrix. With the fiber bridging phenomenon, the fibers bridge each crack in the HPFRC matrix, making cracks difficult to open and causing the cracked section to be stronger than the adjacent uncracked section. Therefore, after additional load is applied, the adjacent uncracked section is forced to crack and distribute the strain along the length of the member, thus preventing yielding of the reinforcement at any section and any associated permanent deflection unlit later in the loading regime.

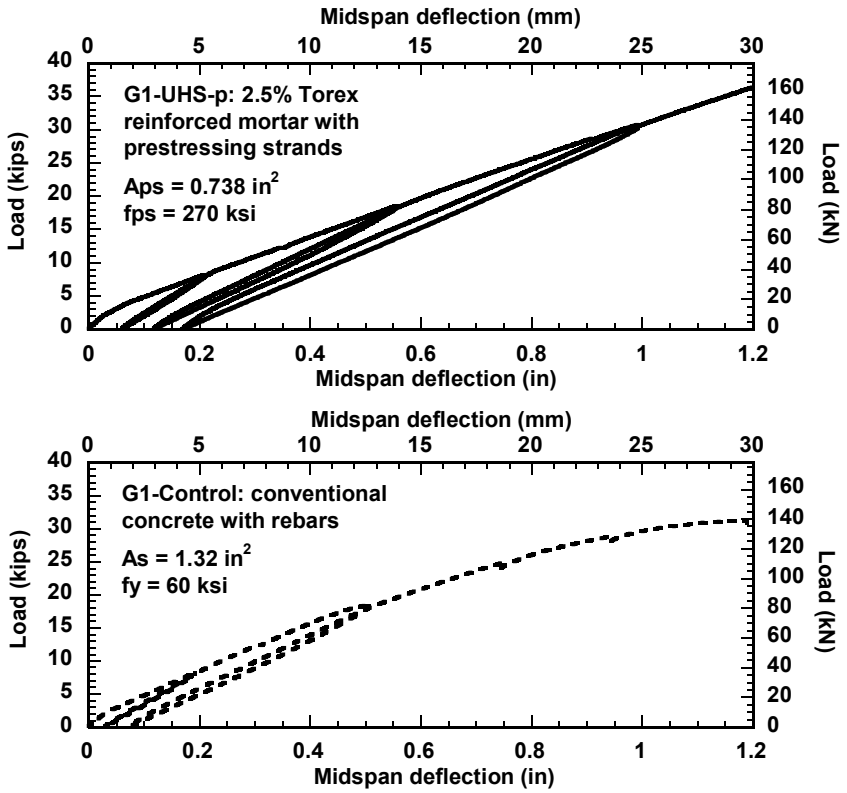

Fig. 6 Initial portion of load versus deflection curve showing loading-unloading of specimens in Group 1 (a) specimen G1-UHS-p (b) specimen G1-Control

After initial cracking, specimens developed more cracks in the maximum positive moment region as the load increased. Fig. 7 shows cracking pattern due to multiple cracking in specimen G1-Control, G1-Tor-p, and G1-UHS-p, respectively. Unlike specimens with HPFRC matrix reinforced with prestressing strands, the conventional RC specimen developed fewer cracks and most cracks are wider.

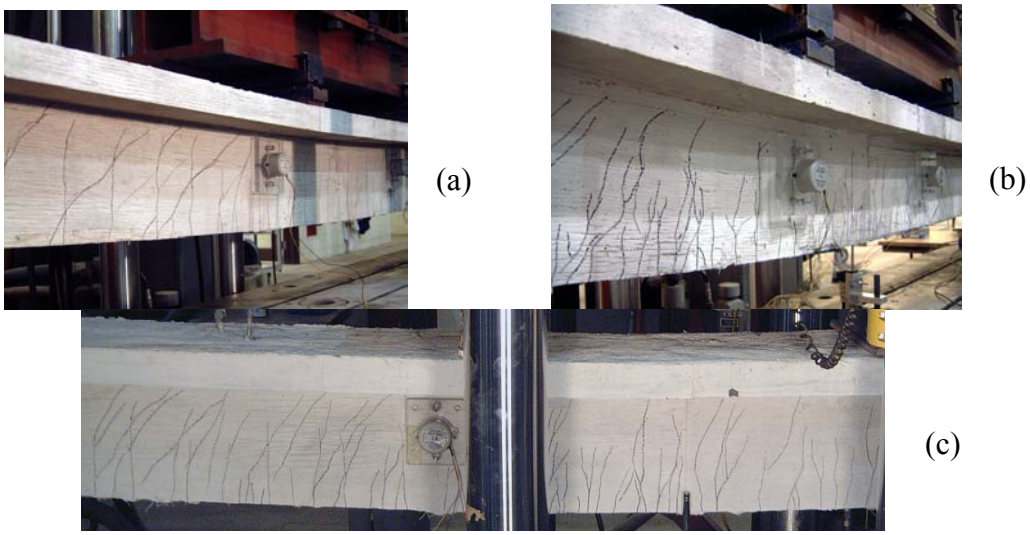

Fig. 7 Cracking pattern before reaching maximum load (a) specimen G1-Control (b) specimen G1-Tor-p (c) specimen G1-UHS-p

Specimens eventually reached the maximum peak load at 51.96, 69.99, and 32 kips for specimen G1-Tor-p, G1-UHS-p, and G1-Control, respectively. This shows that the two specimens representing the proposed concept, one with 2% Torex fiber reinforced mortar and one with UHS mix, exhibits 1.6 and 2.2 times higher load than conventional RC specimen, respectively. This finding; thus, proves that the proposed concept is valid. Also, Fig. 8 shows the deflected shape of specimen G1-UHS-p shortly after maximum load was reached. It is clearly seen that specimen with HPFRC matrix reinforced with prestressing strands shows much more ductile behavior compared to the conventional RC specimen. This visually proves one of the benefits of combining the HPFRC mortar with prestressing strands, as proposed.

Considering the two specimens representing the proposed concept, specimen with UHS mix (2.5% Torex fibers by volume) exhibited higher cracking load as well as higher maximum load compared to specimen with 2% Torex fiber reinforced mortar. This is due to the higher compressive strength as well as higher modulus of rupture of the UHS mix, which then allow higher amount of reinforcement to be placed in the beam while maintaining the ductility.

Finally, all tested specimens failed by compression crushing in the flange. Since all specimens were designed to be closed to the maximum limit of tension controlled section, the reinforcement in each specimen yielded shortly before the compression failure occurred, as seen in the small plateau portion in the load-deflection curve before failure. In the under-reinforced design methodology ($\varepsilon_t < 0.005$ as specified in ACI), a similar behavior is expected with a longer plateau portion in the load-deflection curve before failure, indicating a significant yielding of reinforcement prior to compression failure in the flange. Figures 9(a), (b), and (c) shows the failure section of specimen G1-Tor-p, G1-UHS-p, and G1-Control, respectively. Note that the flange of specimen with conventional concrete was totally crushed into pieces while the failure section of specimen with HPFRC matrix remained intact.

Fig. 8 Deflected shape of specimen G1-Tor-p shortly after reaching maximum load

(a) (b) (c)

Fig. 9 Failure pattern of test specimens (a) specimen G1-Tor-p (b) specimen G1-UHS-p (c) specimen G1-Control

Total Energy-Absorption

In this paper, total energy absorption is defined by the area under the load versus deflection curve up to failure. As seen in Table 5, it is clear that specimen with HPFRC matrix reinforced with prestressing strands exhibited significantly larger energy absorption than the conventional RC specimen, approximately 2 and 2.8 times larger for specimens with 2% Torex fiber reinforced mortar and specimen with UHS mix, respectively. This finding; thus, proves that the proposed concept is valid. By taking advantage of high compressive strength and strain as well as strain-hardening behavior of HPFRC matrix along with high tensile strength of steel strands, a significantly higher ductility compared to a conventional reinforced concrete beam is observed.

Crack Width

Cracks were marked during testing and crack widths were measured periodically throughout the test. The comparison of average crack width in the critical area (constant moment) between the two load points at initial stages is shown graphically in Fig. 10. As expected, the average crack widths measured in proposed beams with HPFRC composites were smaller than in the conventional RC beam made of concrete throughout the test. For the same load level, average crack widths in specimens with HPFRC matrices are smaller by a magnitude

or two. When considering the two specimens representing the proposed concept, specimen with UHS mix (2.5% Torex fibers) shows slightly smaller average crack width compared to specimen with 2% Torex fiber reinforced mortar. At 15 kips (approximately 60% of the maximum load of the control specimen), very fine cracks, as small as 0.08 mm, were observed in both specimens with HPFRC matrices, while an average crack width of 0.15 mm was found in the conventional RC specimen. This is due to the contribution of fiber bridging and emphasizes another advantage of the proposed beam system.

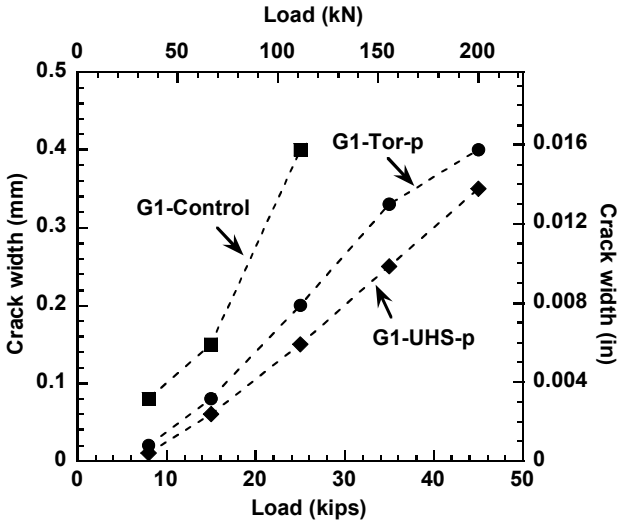

Fig. 10 Comparison of average crack width in the critical area (constant moment) between the two load points of tested specimens in group 1

TEST RESULTS OF CONTINUOUS BEAMS

Load-Deflection Responses

Figures 11(a) and (b) show the load versus deflection curves and load versus rotation responses of all specimens in group 2, respectively. Also, Table 6 presents the summary of the numerical results obtained from tested specimens. In general, all three specimens showed very similar trends, as shown in Figure 11(a). However, control specimens, G2-Control, exhibited inferior performance in term of both strength and ductility.

All specimens behaved elastically before cracking. Similar to simple-span specimen, specimens with 2% Torex fiber reinforced mortar exhibited higher cracking load compared to the control specimen. After cracking, the deflection under the loads started to deviate significantly from linearity as the load increased. More cracks developed in both maximum positive and negative regions as the test progressed. However, unlike specimen with HPFRC matrix, the conventional RC specimen developed only a single crack over the intermediate support and fewer cracks in span. Most cracks are also significantly wider than specimen with HPFRC matrix.

In general, specimens G2-Tor-s and G2-Tor-p behaved similarly after initial cracking; however, specimen G2-Tor-p exhibited a lower inelastic stiffness due to its lower amount of reinforcement. The reinforcing steel in specimen G2-Tor-s yielded at the load of around 21 kips and the load was then stabilized as deflection increased. On the other hand, the prestressing strand in specimen G2-Tor-p has not reached its yield strength at this load level; therefore, the specimen continued to take more load as deflection increased. The prestressing strands in specimen G2-Tor-p finally yielded at the load of approximately 29 kips and the load was then stabilized.

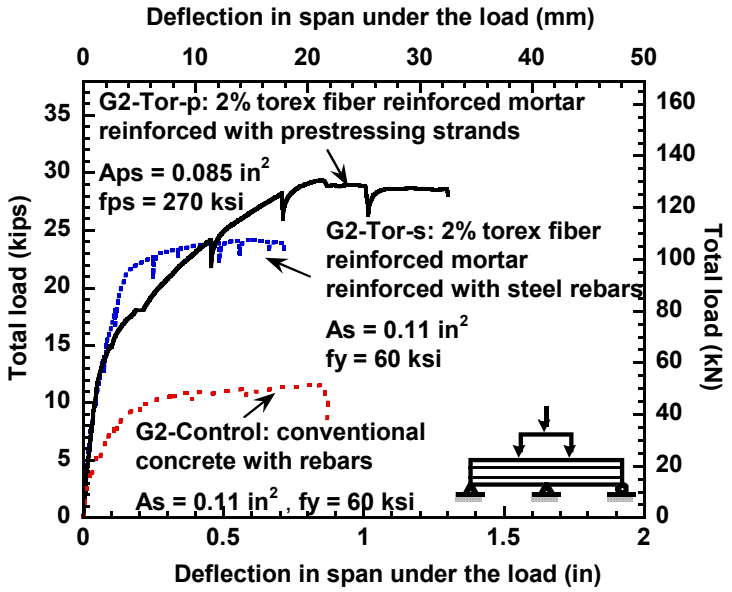

(a)

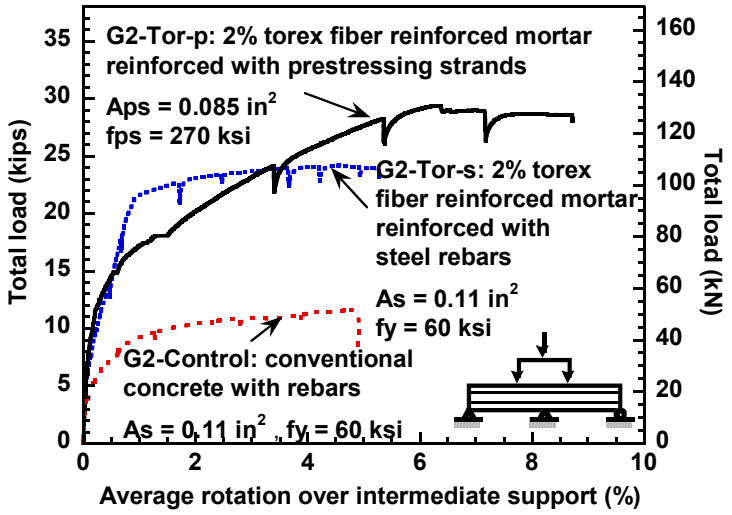

(b)

Fig. 11 (a) Comparison of load-deflection curves of continuous-span test specimens (b) Comparison of load-rotation curves of continuous-span test specimens

Table 6 Summary of the numerical results obtained from tested specimens in group 2

Specimen ID	Cracking load (kips)	Deflection at cracking (in)	Peak load (kips)	Deflection at peak load (in)	Rotation over support at peak load (%)	Maximum rotation over support (%)
G2-Tor-p	5.90	0.032	29.30	0.86	6.34	8.34
G2-Tor-s	5.21	0.037	24.61	0.62	4.55	5.30
G2-Control	3.61	0.016	11.63	0.86	4.83	4.90

Loading – unloading was also done periodically during the beginning of the test. Fig. 12 shows the loading-unloading responses among specimens in Group 2 where Fig. 12(a) shows the permanent deflection and Fig. 12(b) shows the permanent rotation after unloading, respectively. Unloading at the load of about 7 kip (60% of the predicted maximum load of the control specimen) shows that specimens with proposed concept exhibited significantly smaller permanent deflection as well as rotation when unloading. This is expected since, unlike conventional concrete, cracks in HPFRC composites are very fine at this early stage. They tend to close completely after unloading due to fiber bridging. In addition, unloading at higher load (15 kips) for both specimens with proposed concept also shows very small permanent deflection and rotation over the intermediate support. No different in permanent deflection and rotation was observed between specimen reinforced with rebar and specimen reinforced with unstressed prestressing strand at this load level.

In specimens with HPFRC matrix, the plastic hinge mechanism associated with typical continuous beams can be seen clearly by the cracking pattern in the specimen. The cracking pattern showed cracks clustered around the area where the reinforcements yielded, indicating the formation of two plastic hinges in the maximum negative moment region (over the intermediated support) and in the maximum positive moment region (under the point load). Fig. 13 shows the multiple cracking pattern in specimen with HPFRC matrix compared to conventional concrete specimen.

Eventually, the specimens reached the maximum load. As seen in Table 6, specimens G2-Tor-p and G2-Tor-s exhibits approximately 2.5 times and 2 times higher load than specimen G2-Control, respectively. In addition, considering different types of reinforcement in specimens with HPFRC matrix, specimen reinforced with prestressing strands exhibited higher load and higher deflection compared to specimen reinforced with rebars. This is due to a higher yield strength of prestressing strand which allow the specimen to take more load as the deflection increased. This proves another benefit of combining the high compressive/tensile strain of HPFRC mortar with high tensile strength (which corresponds to high yield strength) of the prestressing strands, as proposed.

In term of rotation, as shown in Fig. 11(b), for the same rotation, specimen with HPFRC mortar reinforced with steel rebars showed significant higher load compared to the control specimen, indicating an enhancement from fibers. After the yielding of the steel reinforcement in all specimens, the load was stabilized as the rotation increased significantly. Note that after reaching maximum load, specimens with HPFRC mortar reinforced with

prestressing strands as well as with steel rebar maintained high loads up to a rotation of as high as 8% and 5.3%, respectively. This is due to the contribution of fiber bridging. On the other hand, the control specimen exhibited a lower maximum rotation of 4.9% as the shear failure occurred.

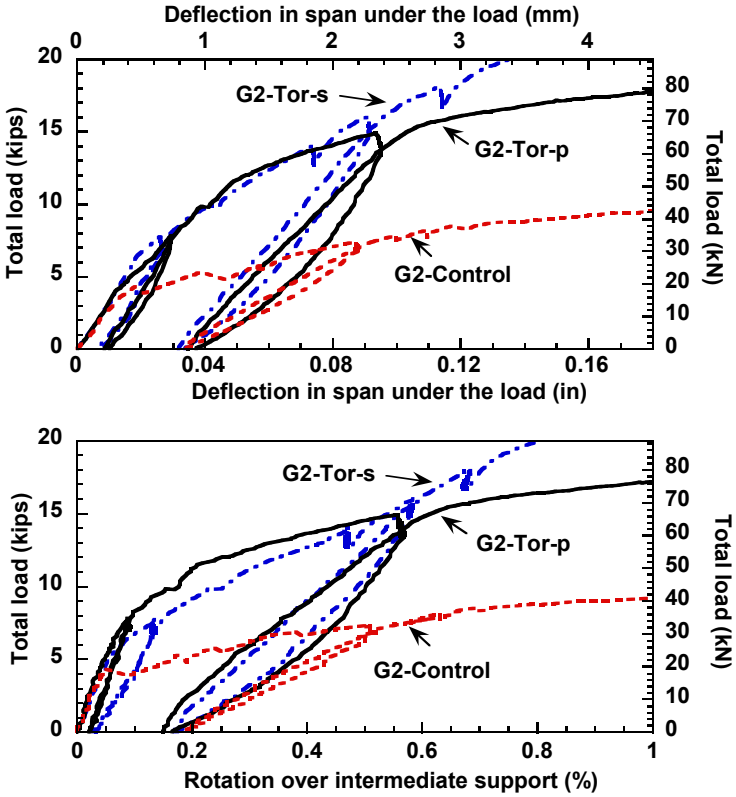

Fig. 12 Loading-unloading responses among specimens in Group 2 (a) the permanent deflection after unloading (b) the permanent rotation over the intermediate support after unloading

Ultimately, load in all specimens was stabilized and cracks opened wider over the support as the deflection increased. For specimens with HPFRC matrix, the test was stopped after a large crack opening (more than 0.5 in. or 12 mm) was observed over the intermediate support. Note that at the end of the test, load still stabilized as the cracks opened wider over the intermediate support, indicating a ductile behavior of this system. Fig. 14(a) shows the cracking pattern over the intermediate support of specimen with HPFRC matrix at the end of the test. For the control specimen, a shear failure occurred over the intermediate support, as shown in Fig. 14(b), and the load dropped sharply. The failure was sudden and brittle. The test was then stopped.

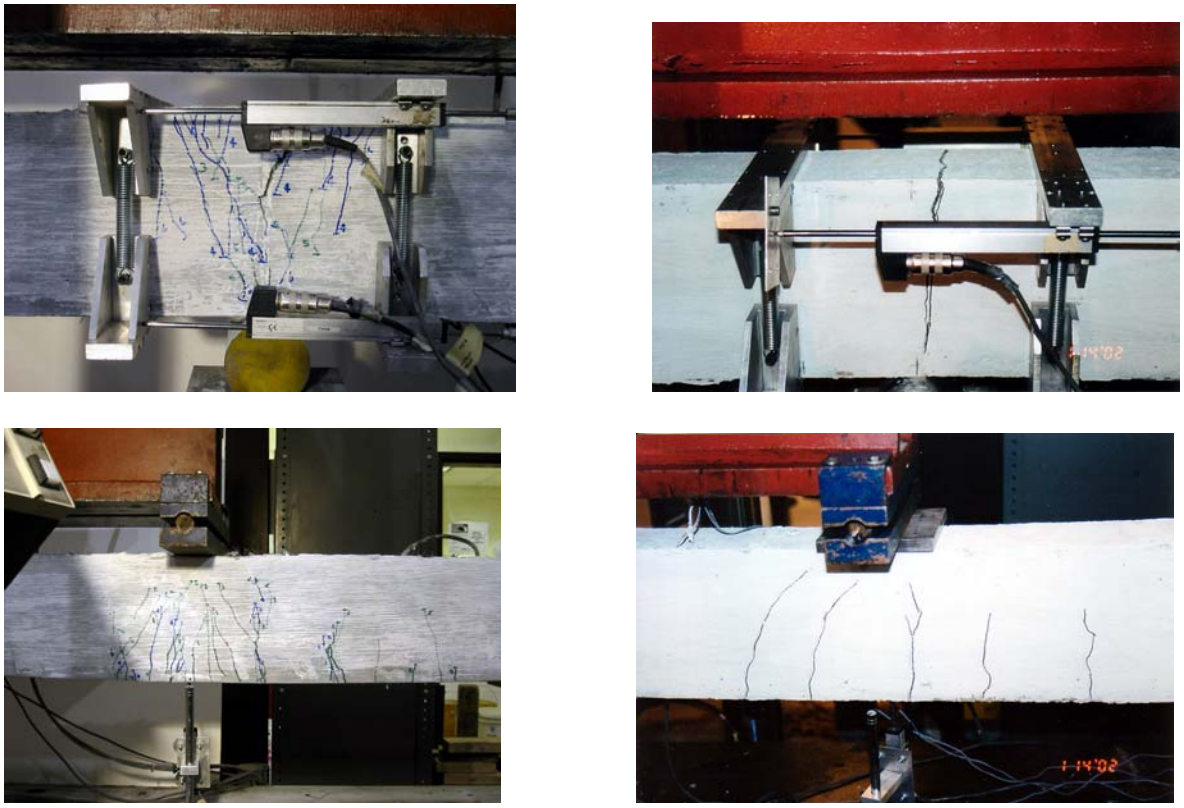

(a) (b)

Fig. 13 Cracking pattern in the maximum negative and positive moment regions (a) specimen with HPFRC matrix reinforced with prestressing strands (b) conventional RC specimen with concrete

Fig. 14 (a) Crack opened wide over the intermediate support of specimen with HPFRC matrix before the test was stopped (b) Shear failure in conventional RC specimen

Energy-Absorption

Energy absorption is defined here as the area under the load versus deflection curve. Fig. 15 shows a comparison of energy absorption among specimens in group 2, it was plotted at every 0.1 in deflection up to 0.8 in (the failure of a control specimen). All specimens exhibited similar energy absorption up to the deflection of 0.1 in. After that, both specimens with HPFRC mortar showed significant higher energy absorption up to failure compared to conventional RC specimen. This is due to the contribution of fiber in the matrix as the crack starts to form. This shows another advantage of using HPFRC matrix.

For specimen with HPFRC mortar, specimen reinforced with prestressing strands showed approximately the same energy absorption as specimen reinforced with steel rebars; however, after reaching a deflection of 0.7 in, a slightly higher energy absorption was observed in specimen reinforced with prestressing stands. This is due to a higher yield strength of prestressing strands which allow the specimen to take more load as the deflection increased, even beyond a deflection of 0.7 in. This confirms another benefit of combining the HPFRC mortar with prestressing strands.

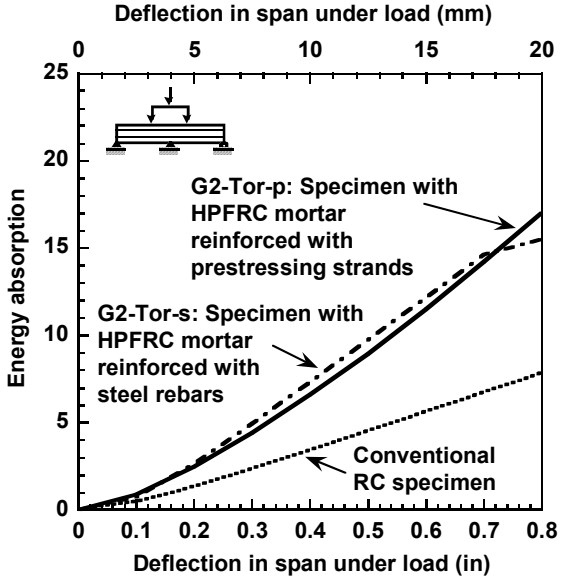

Fig. 15 Comparison of energy absorption among specimens in group 2

Crack Width

Fig. 16 shows the average crack widths measured at each stage over the intermediate support. Due to the effect of fiber bridging, the average crack widths measured in specimens with HPFRC composites were smaller than in the conventional RC beam made of concrete throughout the test. At the load of 6 kips (approximately 60% of the maximum load of the control specimen), a crack in the conventional RC specimen was 0.5 mm wide. Note that

only one crack was found over the intermediate support. On the other hand, significantly finer cracks, less than 0.1 mm, were found in specimens with HPFRC matrix.

Considering two different reinforcements in specimen with HPFRC matrix, average crack widths in specimen reinforced with steel rebars are of the same magnitude as specimen reinforced with prestressing strand; however, once the steel rebars yields, larger cracks were observed in specimen with rebar reinforcement.

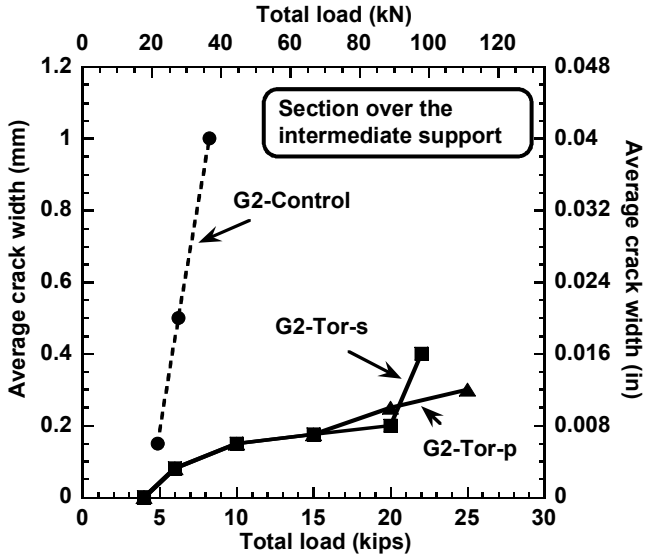

Fig. 16 Comparison of average crack width over the intermediate support among specimens in group 2.

In summary, based on the results from both simple span and continuous span beam tests, the presence of a HPFRCC matrix combined with prestressing strands, as proposed here, contributes to a better performance of the structure in term of both strength and ductility compared to the conventional RC beam. The smaller crack width by a magnitude or two was also observed in the beam with the proposed concept due to the effect of fiber bridging the crack in the HPFRC matrix, thus implying significantly better long-term durability.

CONCLUSIONS

1. The proposed concept in which a high tensile strength prestressing strand is used in combination with a HPFRCC matrix, works as anticipated, that is, it contributes to significantly higher strength and superior structural ductility.
2. Significantly smaller crack width was observed in specimens with the proposed system due to the presence of fiber in the matrix; this should help minimize ingress of corrosive agents and promote a longer service life of the structure.
3. At a reinforcement close to the maximum limit of tension-controlled section (as defined by ACI), the two beams representing the proposed concept, one with 2% Torex fiber

reinforced mortar (f'_c = 8.6 ksi) and one with UHS mix (f'_c = 14.1 ksi), had a maximum load 1.6 and 2.2 times and an energy absorption capacity about 2 and 2.8 times that of the control specimen, respectively. They also had a slightly higher load at first cracking.

4. Specimen with UHS mix (2.5% Torex fibers by volume) exhibited higher cracking load, higher maximum load, as well as higher energy absorption compared to specimen with 2% Torex fiber reinforced mortar due to the higher compressive strength as well as higher modulus of rupture of the UHS mix, which then allow higher amount of reinforcement to be placed in the beam while maintaining the ductility.

5. In a continuous-span beam with low reinforcement ratio, the specimens with 2% Torex fiber reinforced mortar showed a maximum load ranging from 2 to 2.5 times (depending on the type of reinforcement) the maximum load achieved by the conventionally reinforced concrete specimen.

6. Beam specimens with HPFRC matrix reinforced with prestressing strands exhibited a maximum load higher than beams with same reinforcement ratio of conventional reinforcing bars.

7. In the two-spans continuous beams reinforced with prestressing strands and a HPFRC matrix, a rotation over the intermediate support as high as 8% was observed while the load was still maintained closed to the maximum load.

ACKNOWLEDGMENTS

This research was supported in part by a grant from the National Science Foundation (CMS 0096700) with Dr. P. Chang as Program Director. The authors also acknowledge the support of the University of Michigan, College of Engineering, under the Infrastructure Systems Initiative program. Any opinions, findings, and conclusions expressed in this study are those of the authors, and do not necessarily reflect the views of the sponsors.

REFERENCES

1. Reinhardt, H.W., and Naaman, A.E., 'High Performance Fiber Reinforced Cement Composites', RILEM, Vol. 15, E. & FN Spon, London, 1992, 565 pages.

2. Naaman, A.E., and Reinhardt H.W., 'High Performance Fiber Reinforced Cement Composites - HPFRCC 2', RILEM Proceedings 31, E. & FN Spon, London, 1996, 502 pages.

3. Reinhardt, H.W., and Naaman, A.E., 'High Performance Fiber Reinforced Cement Composites- HPFRCC 3', PRO 6, RILEM Publications S.A.R.L., Cachan, France, May 1999, 666 pages.

4. Fanella, D., and Naaman, A.E., 'Stress-Strain Properties of Fiber Reinforced Mortar in Compression', *ACI Journal*, Vol. 82, No. 4, July/August 1985, pp. 475-483.

5. Naaman, A.E., Reinhardt, H.W., Fritz, C. and Alwan, J., 'Nonlinear Analysis of RC Beams Using a SIFCON Matrix', *Materials and Structures*, Vol. 26, RILEM, France, 1993, pp. 522-531.

6. Naaman, A.E., 'New Fiber Technology: Cement, Ceramic and Polymeric Composites',

Concrete International, Vol. 20, No. 11, July 1998.

7. Sujiravorakul, C., 'Development of High Performance Fiber Reinforced Cement Composites Using Twisted Polygonal Steel Fibers', Ph.D. Dissertation, University of Michigan, Ann Arbor, 2001.

8. ACI Committee 318, *Building Code Requirements for Reinforced Concrete and Commentary, ACI 318R-95*, American Concrete Institute, Farmington Hills, 1995.

9. Naaman, A.E., and Chandrangsu, K., 'Innovative Bridge Deck System Using High Performance Fiber Reinforced Cement Composites', *ACI Structural Journal*, Vol. 101, No. 1, Jan-Feb, 2004, pp. 57-64.

10. Chandrangsu, K., and Naaman, A.E., 'Experimental Testing of Innovative Bridge Decks with Reduced Reinforcement and Strain-Hardening Fiber Reinforced Cementitious Composites', *6th RILEM Symposium on fiber reinforced concretes BEFIB 2004*, in Varenna-Lecco, Italy, 20-22 September 2004.